The American Journal of Pathology, Vol. 189, No. 7, July 2019

The American Journal of
PATHOLOGY
ajp.amjpathol.org

CELL INJURY, REPAIR, AGING, AND APOPTOSIS

Ubiquitin-Specific Protease 15 Maintains Transforming Growth Factor-β Pathway Activity by Deubiquitinating Transforming Growth Factor-β Receptor I during Wound Healing

Yixuan Zhao, Zi Wang, Chiakang Ho, Guoyou Zhang, and Qingfeng Li

From the Department of Plastic and Reconstructive Surgery, Ninth People's Hospital, Shanghai Jiao Tong University School of Medicine, Shanghai, People's Republic of China

Accepted for publication March 5, 2019.

Address correspondence to Guoyou Zhang, M.D., Ph.D., or Qingfeng Li, M.D., Ph.D., Department of Plastic and Reconstructive Surgery, Ninth People's Hospital, Shanghai Jiao Tong University School of Medicine, 639 Zhizaoju Rd., Shanghai 200011, China. E-mail: guoyou.zhang@sh9hospital.org or dr.liqingfeng@shsmu.edu.cn.

Wound healing is a process of cutaneous barrier reconstruction that occurs after skin injury and involves diverse cytokines and cell types. Similar to several deubiquitinating enzymes, ubiquitin-specific protease 15 (*USP15*) can remove ubiquitin chains from specific proteins to rescue them from degradation. However, the regulatory role of USP15 in wound healing remains unclear. We investigated the dynamic function of USP15 in wound healing. First, in *USP15* knockout mice, we observed a significant delay in wound closure. In addition, inhibition of cell proliferation and migration was observed in USP15-silenced human dermal fibroblasts. Through RNA sequencing, it was revealed that the transforming growth factor-β (TGF-β) pathway was suppressed after *USP15* knockdown. Furthermore, coimmunoprecipitation demonstrated that USP15 could interact with TGF-β receptor I and promote its deubiquitination, thereby maintaining TGF-β signaling pathway activity by enhancing TGF-β receptor I stability. These observations shed light on the function and mechanisms of USP15-mediated modulation of the TGF-β signaling pathway during wound healing, thus providing a novel potential target for the treatment of refractory wounds. *(Am J Pathol 2019, 189: 1351–1362; https://doi.org/10.1016/j.ajpath.2019.03.005)*

Wound healing is an intricate and complicated process that occurs after tissue injury and involves reciprocal actions and reactions among diverse cells, growth factors, cytokines, and extracellular matrix (ECM) components.[1] This process relies on the appropriate coordination of multiple cell types in the dermal layer, such as fibroblasts, immune cells, and epidermal cells, including keratinocytes.[2] During the three distinct but overlapping phases of wound healing (inflammation, proliferation, and tissue remodeling), dermal fibroblasts play a critical role by secreting cytokines that mediate cellular communication.[3] Dermal fibroblasts participate in ECM deposition and function by regulating the dynamic interplay among cell types from distinct sources at the same time.[4] Therefore, dermal fibroblasts play a key role in the process of skin wound repair.

Among the various growth factors involved in both wound healing and fibroblast function, transforming growth factor β1 (TGF-β1) is believed to play a major biological role in these processes.[5] A previous study helped elucidate the vital role of the TGF-β signaling pathway in promoting wound healing by regulating various cellular responses, including cell proliferation, migration, ECM synthesis, and reepithelization.[6] However, excessive amounts of TGF-β1 can also

Supported in part by the National Natural Science Foundation of China grants 81571904 (G.Z.) and 81620108019 (Q.L.) and the Scientific Research Foundation for Returned Overseas Chinese Scholars of the State Education Ministry project 201550005 (G.Z.).

Y.Z. and Z.W. contributed equally to this work.

G.Z. and Q.L. contributed equally to this work as senior authors.

Disclosures: None declared.

https://doi.org/10.1016/j.ajpath.2019.03.005

lead to overhealing outcomes, such as hypertrophic scars or keloid formation.[7] Moreover, the TGF-β signaling pathway is known to be regulated by ubiquitin-regulated proteolysis.[8] Given that human dermal fibroblasts (HDFs) are sensitive to TGF-β1, elucidation of the specific mechanisms by which TGF-β1 acts on HDFs during wound healing is important.

As one of the major post-translational modifications of the TGF-β pathway in proteasome degradation, ubiquitination is a reversible protein modification process.[9] Ubiquitination participates in diverse aspects of disease development, such as oncogenesis and immune reactions.[10] During ubiquitination, target proteins can be targeted to the proteasome, which leads to proteolysis.[11] This reversible process can be terminated by deubiquitinating enzymes (DUBs) via removal of the ubiquitin chains from targeted proteins awaiting degradation,[12] which involves specific cleavage of both the ubiquitin chains and the protein substrates.[13] For example, a previous study reported that ubiquitin-specific protease 4 (*USP4*) and ubiquitin-specific protease 15 (*USP15*) can regulate TGF-β pathway activity, which enhances the stability of ubiquitinated receptors against the negative effects of receptor-ubiquitinating complexes.[9]

Specifically, USP15 can directly bind to receptor-phosphorylated SMAD proteins and deubiquitinate TGF-β receptor I (TBR1), thereby promoting its stability and up-regulating the TGF-β signaling pathway.[14] In addition, USP15 participates in many pathophysiological processes and functions in combination with interferons and E3 ligases, such as mouse double minute 2 (MDM2) and Kelch-like ECH associated protein 1 (Keap1), thereby regulating neuroinflammation, T-cell activation, and antioxidant responses.[15–17] Previous studies have also emphasized the potential functions of USP15 in the maintenance of the TGF-β signaling pathway[9]; however, the regulatory role of *USP15* in wound repair remains unclear.

Herein, we first investigated the regulatory role of USP15 in wound rehabilitation via *USP15* knockout (KO) mice. USP15 promoted HDF proliferation and migration. Moreover, USP15 could deubiquitinate and stabilize TBR1, thereby maintaining TGF-β levels. Our study conclusively identifies a novel mechanism in which USP15 regulates TGF-β–guided wound repair and provides alternative therapeutic targets for wound healing.

Materials and Methods

Animal Model

All animals were cared for and used in accordance with the appropriate guidelines. The protocol received ethical approval from the Independent Ethics Committee of Shanghai Ninth People's Hospital (Shanghai, China). *USP15* KO mice were purchased from Nanjing Biomedical Research Institute of Nanjing University (Nanjing, China). The single-guide RNA sequences used to establish the USP15 KO mice are listed in Table 1.

Table 1 Sequence of sgRNAs Used in Establishing *Usp15*$^{-/-}$ Mice

sgRNAs	sgRNA sequence	PAM
Usp15-S1	5′-CCTGGACCCATCGATAACTC-3′	TGG
Usp15-S2	5′-AGCTGGGACAAATACCAGAT-3′	GGG

PAM, protospacer adjacent motif; S1, sequence 1; S2, sequence 2; sgRNA, single-guide RNA.

USP15 KO and wild-type (WT) mice with a C57BL/6 background were bred under specific pathogen-free conditions. Genotypes were confirmed by native PAGE. Both the *USP15* KO and WT groups included eight female and six male mice. Mice, aged 8 to 10 weeks, were anesthetized by i.p. injection, sterilized with alcohol, and shaved at the dorsum. Two 5-mm–diameter full-thickness cutaneous wounds were generated by a biopsy punch on both sides along the midline of the mouse. The wound area was measured from day 1 to day 7 using ImageJ software version 1.50i (NIH, Bethesda, MD; *http://imagej.nih.gov/ij*) in a blinded manner (C.H.). The qualitative data were measured and quantified by another investigator who was not the experiment operator (Y.Z.). Wounded tissue specimens were collected on the appropriate days after injury and fixed in 4% paraformaldehyde for embedding in paraffin.

Histology, Immunohistochemistry, and Immunofluorescence

Wounded skin tissue sections, embedded in paraffin, were stained with hematoxylin and eosin or Masson trichrome, as previously described.[18] Epithelial thickness and epithelial gaps were measured from hematoxylin and eosin–stained slides using ImageJ software. For the immunofluorescence assay, fibroblasts growing on slides were fixed in 4% paraformaldehyde for 10 minutes at room temperature. After the cells were washed in phosphate-buffered saline, they were treated with primary antibodies specific for USP15 (dilution 1:200; 14354-1-AP; Proteintech, Rosemont, IL) and SMAD7 (dilution 1:50; sc101152; Santa Cruz Biotechnology, Dallas, TX) at 4°C overnight. Fluorescein isothiocyanate– and Alexa Fluor 546–conjugated secondary antibodies (dilution 1:200; A24538 and A10036, respectively; Invitrogen, Waltham, MA) were used to detect the primary antibodies. Then, DAPI was used for nuclear counterstaining. Images were captured and analyzed using NIS-Elements BR software version 4.50.00 (Nikon, Tokyo, Japan) on a Nikon Eclipse-Ni-U microscope (Nikon).

TGF-β1 Enzyme-Linked Immunosorbent Assay of Peripheral Blood

Peripheral blood from *USP15*$^{+/+}$ and *USP15*$^{-/-}$ mice was collected from the posterior orbital veniplex. Serum was

obtained after centrifugation at 8000 × *g* for 15 minutes. A total of 40 μL of clear serum per sample was assayed using a TGF-β1 enzyme-linked immunosorbent assay kit (KE10005; Proteintech), according to the manufacturer's instructions.

Cell Culture

HDFs originating from neonatal foreskin were purchased from the Stem Cell Bank of the Chinese Academy of Sciences (Beijing, China). The cells were cultured in a humidified atmosphere at 37°C with 5% CO_2 using Dulbecco's modified Eagle's medium/high glucose (Gibco, Waltham, MA) with 10% fetal bovine serum (Gibco) and 1% penicillin (100 U/L)—streptomycin (100 mg/L) (Gibco). The cells were transfected with lentivirus at the third passage after resuscitation. Stable USP15-silenced cells were established at the fifth passage. Further experiments were performed between the sixth and eighth passages. HDFs were treated in the absence or presence of 100 ng/mL recombinant human TGF-β1 (240-B-002; R&D Systems, Minneapolis, MN) for 24 hours after transfection with lentivirus.

Lentivirus Transfection

The three siRNAs targeting *USP15* were initially designed in the RNA interference designer platform (Thermo Fisher Scientific, Waltham, MA) and subsequently selected. The RNA silencing efficiency was confirmed by real-time PCR, and the two siRNAs with the best knockdown efficiency were selected and cloned into the GPH vector. HEK293T cells were used to produce lentivirus by transfecting USP15-shRNA plasmids together with pMD2.D plasmids and PsPax plasmids. Forty-eight hours after transfection, the supernatant was collected and filtered for further infection. The cells were infected at 30% to 40% confluence in the presence of lentiviral supernatant and normal medium at a 1:1 dilution with 10 ng/mL polybrene (Sigma, St. Louis, MO) using standard techniques. Empty GPH vector served as a negative control. The shRNA sequences are listed in Table 2.

Quantitative Real-Time PCR and RNA Sequencing

RNA was extracted from skin tissue and fibroblasts using TRIzol Reagent (Invitrogen), according to the manufacturer's protocols. Quantitative real-time PCR was performed according to standard techniques. Glyceraldehyde 3-phosphate dehydrogenase (*GAPDH*) served as the endogenous control. The primers are listed in Table 3. RNA was sequenced and analyzed by Kangcheng Bio-tech Inc. (Shanghai, China).

Table 2 Sequence of shRNAs Used in the Experiment

shRNA	Sequence
sh*USP15*-1	5′-GATACAGAGCACGTGATTATT-3′
sh*USP15*-2	5′-GGAATGGCCCAAATGGCATAC-3′

Table 3 Primers Used for qPCR

Gene	Sequence
Usp15	F: 5′-ACGTTGCTGTGAGGACCAGA-3′
	R: 5′-GCTCTTGATCCTGGCTGGAC-3′
USP15	F: 5′-AAAACCTCGCTCCGGAAAGG-3′
	R: 5′-CCACCTTTCGTGCTATTGG-3′
Tgfb1	F: 5′-GCAACAATTCCTGGCGTTACCTTG-3′
	R: 5′-CCTGTATTCCGTCTCCTTGGTTCAG-3′
TGFB1	F: 5′-AGAACTTCCAACTACTGGCCC-3′
	R: 5′-TTCTTCTCCCCGCCACTTTC-3′
Tbr1	F: 5′-CATTGCTGGTCCAGTCTGCTTCG-3′
	R: 5′-TGGTGAATGACAGTGCGGTTATGG-3′
SERPINE1	F: 5′-TCCACAAATCAGACGGCAGC-3′
	R: 5′-ATGATGATCTCCTCGGGGGC-3′
Gapdh	F: 5′-TGTGAACGGATTTGGCCGTA-3′
	R: 5′-GTCTCGCTCCTGGAAGATGG-3′
GAPDH	F: 5′-GGGAAGGTGAAGGTCGGAGT-3′
	R: 5′-GGGGTCATTGATGGCAACA-3′

F, forward; qPCR, quantitative real-time PCR; R, reverse.

Western Blot Analysis

Cells grown to 80% confluence were lysed in radioimmunoprecipitation assay buffer with protease inhibitor cocktails (R0010 and P6730; Solarbio, Beijing, China). Western blot analysis was performed, as previously described.[18] The following primary antibodies were used: USP15 (dilution 1:1000; 14354-1-AP; Proteintech), serpin family E member 1 (SERPINE1; dilution 1:1000; catalog number 11907; Cell Signaling, Danvers, MA), TBR1 (dilution 1:1000; 20932-1-Ap; Proteintech), SMAD2/3 (dilution 1:1000; catalog number 5678; Cell Signaling), phosphorylated SMAD2/3 (dilution 1:500; sc11769; Santa Cruz Biotechnology), SMAD7 (dilution 1:500; sc101152; Santa Cruz Biotechnology), SMAD1/5 (dilution 1:1000; catalog number 12656; Cell Signaling), SMAD4 (dilution 1:1000; catalog number 38454; Cell Signaling), and ubiquitin (dilution 1:1000; catalog number ab19247; Abcam, Cambridge, UK). Horseradish peroxidase—conjugated secondary antibody was detected by electrochemiluminescence reagent (catalog number PE0020; Solarbio). Band signals were visualized using an Amersham Imager 600 (General Electric Company, Boston, MA).

Cell Counting Kit-8 Assay

Cell proliferation was determined by Cell Counting Kit-8 (Dojindo, Tokyo, Japan). Cells transfected with shRNAs were seeded in 96-well plates at a density of 3×10^3 cells per well, and Cell Counting Kit-8 solution was added on days 0, 1, 3, and 5 to measure the OD at 450 nm.

Every experiment was repeated independently at least three times.

Scratch Assay

For cell migration analysis, a scratch assay was used to imitate the wound closure process. Plated fibroblasts were grown to confluence in 6-well plates and serum starved for 24 hours before scratching. A scratch was made through the diameter of each well using plastic pipette tips. Images were taken using a Nikon Eclipse-Ti-S microscope (Nikon). The width between the two edges of the scratch was measured using ImageJ software. The measurement was performed in a blinded manner (C.H.), and the investigator (Y.Z.) measured the gap without knowing which treatment group was being analyzed.

Transwell Assay

Transwell assays were performed using hanging cell culture inserts (8-μm pore size; Millipore, Burlington, MA) in 24-well plates. A total of 2×10^4 fibroblasts were seeded after overnight starvation and harvested 24 hours later. The upper cells in the filters were gently removed with a cotton swab, whereas cells that migrated to the other side were stained with 0.5% crystal violet. Images of three random fields from each insert were captured, and the cell numbers in each field were counted.

Flow Cytometry/Cell Cycle Analysis

Cell cycle assays were performed using PI/RNase Staining Buffer (550825; BD Pharmingen, Franklin Lakes, NJ). A total of 1×10^6 cells were collected and fixed in 75% alcohol at −20°C overnight. After the cells were centrifuged and washed twice with phosphate-buffered saline, they were resuspended in 500 μL of propidium iodide and incubated for 15 minutes in the dark at room temperature. The cells were then analyzed by flow cytometry.

Co-IP Assay and Immunoblotting

HDFs treated with or without 100 ng/mL human recombinant TGF-β1 were harvested with IP Lysis/Wash Buffer (Thermo Fisher Scientific). The supernatant was collected after centrifugation at 13,000 × *g* for 10 minutes for protein concentration determination. Lysate (1 mg) was used for co-immunoprecipitation (Co-IP). Immunoprecipitation was performed according to the manufacturer's instructions using a Thermo Fisher Scientific Pierce Co-IP Kit (26149; Thermo Fisher Scientific). Different antibodies, as described above, including USP15 (dilution 1:100), SMAD7 (dilution 1:50), TBR1 (dilution 1:100), and ubiquitin (dilution 1:100) antibodies, were used for immunoprecipitation. The bait and prey proteins were incubated with gentle mixing overnight at 4°C. The protein mixtures were then separated by SDS-PAGE.

Statistical Analysis

The results are expressed as the means ± SEM. Statistical differences were determined by unpaired *t*-tests and one-way analysis of variance, when appropriate. The GraphPad Prism 6 (GraphPad Software, San Diego, CA) program was used for statistical calculations. Differences were considered statistically significant when $P < 0.05$.

Results

Usp15 Deficiency Results in Delayed Wound Closure *in Vivo*

First, a *Usp15* KO mouse was established with a 40-bp deletion in the second exon of *Usp15* (Figure 1A). A wound-healing model was constructed using full-thickness wounds in *Usp15* KO and *Usp15* WT ($Usp15^{+/+}$) mice. The wound closure rate was measured by assessing the area of the wound over 5 days after injury. From a general view of wounds on the dorsal skin, wound closure was found to be significantly delayed in both male and female $Usp15^{-/-}$ mice compared with that in $Usp15^{+/+}$ mice (Figure 1, B and C). Notably, there was no significant difference between sexes in *Usp15* KO or WT mice.

Sections of wounded skin were subsequently harvested over 7 days. The area of the wounded region was measured to determine the reepithelization rate, and epithelial thickness was also analyzed. Hematoxylin and eosin staining showed that the epithelial thickness was significantly decreased in *Usp15*-deficient mice, and the recovery rate, represented by the width of the epithelial gap, was significantly restricted compared with that of WT mice (Figure 1, D–F). In addition, Masson staining revealed that the collagen level in *USP15*-deficient dermal skin was lower than that in WT skin (Figure 1G). These results showed that wound recovery is delayed in *USP15*-deficient mice, demonstrating that silencing *USP15* attenuates wound healing *in vivo*.

USP15 Knockdown Attenuates Cell Migration and Proliferation in HDFs

Because dermal fibroblasts are essential for cutaneous damage repair, the role of *USP15* in HDFs was studied. First, USP15-silenced HDFs were established through shRNA. shRNA lentivirus targeting USP15 with enhanced green fluorescent protein was transfected into HDFs (Figure 2A). As expected, *USP15* was down-regulated after shRNA interference at both the RNA (Figure 2, B and C) and protein (Figure 2D) levels. Furthermore, a scratch assay (Figure 2, E and F) was used to simulate wound healing in cells. Together with the transwell assay data, the results

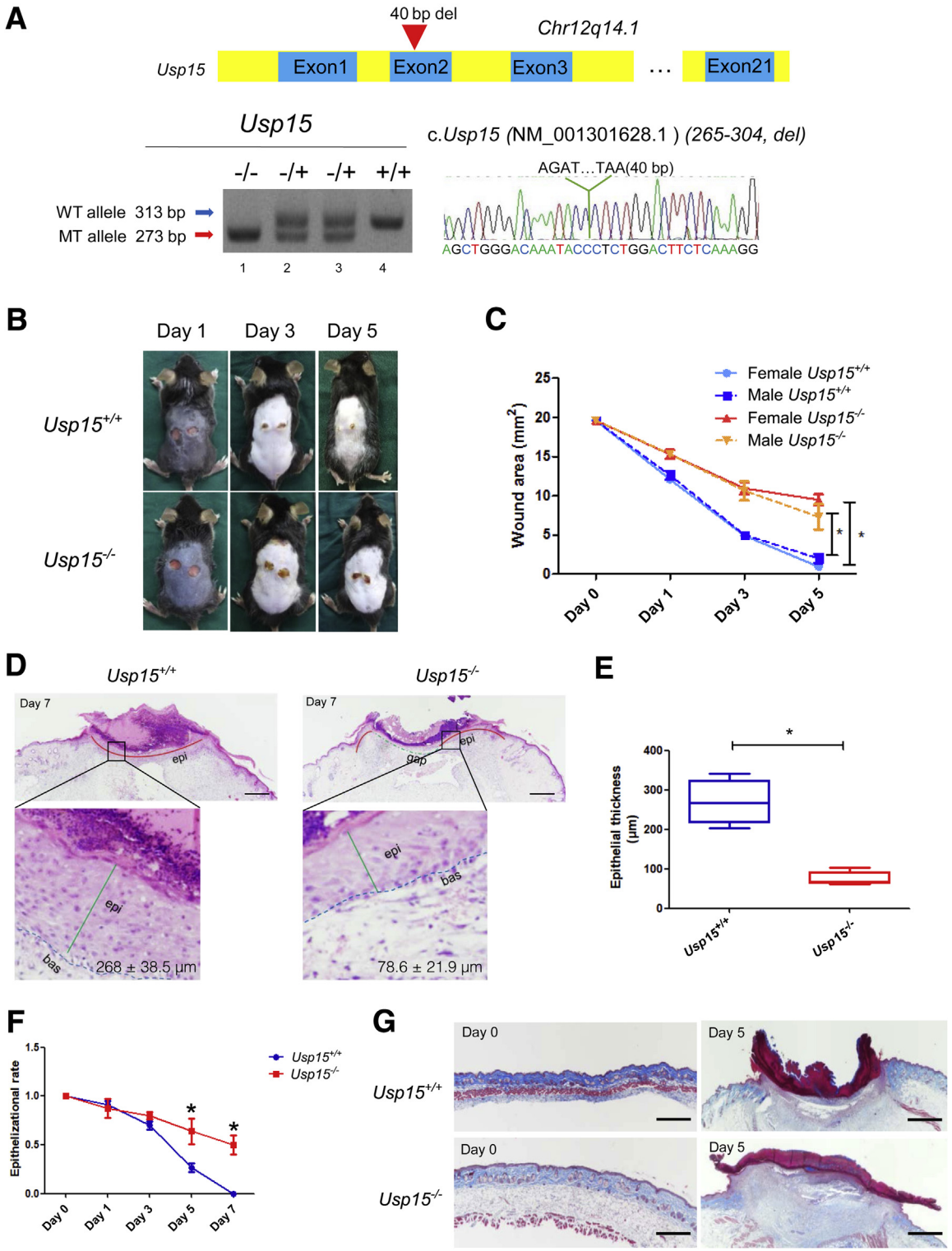

Figure 1 Wound healing is delayed in *Usp15*-deficient mice. **A:** Establishment of *Usp15* knockout mice. A 40-bp region of the second exon of *Usp15* was deleted (c. Usp15: 265-304 del). Genotyping was performed for further identification. **B:** Full-thickness wounds (5-mm diameter) were made on the dorsal skin of $Usp15^{+/+}$ and $Usp15^{-/-}$ mice. Images of dorsal skin were taken from day 1 to day 5. **C:** The wound area was measured to estimate the wound contraction rate. **D:** Biopsy sections were collected over 7 days after injury. Hematoxylin and eosin staining was used to assess epithelial thickness and epithelial gaps. **Dashed blue lines** indicate basal layer (bas); **red lines**, epidermis (epi); **solid green lines**, thickness of epidermis; **dashed green line**, the gap between re-epithelial wound area. **E** and **F:** Quantification of epithelial thickness (**E**) and the width of the epithelial gap (**F**). The width of the epithelial gap represents the epithelization rate. **G:** Masson staining shows that collagen expression is down-regulated in the skin of $Usp15^{-/-}$ mice. $n = 6$ male $Usp15^{+/+}$ and male $Usp15^{-/-}$ (**C**); $n = 8$ female $Usp15^{+/+}$ and female $Usp15^{-/-}$ (**C**); $n = 6$ to 8 for each sex and time point (**E** and **F**). *$P < 0.05$ versus $USP15^{+/+}$. Scale bars = 100 μm (**D** and **G**). MT, mutant type; WT, wild type.

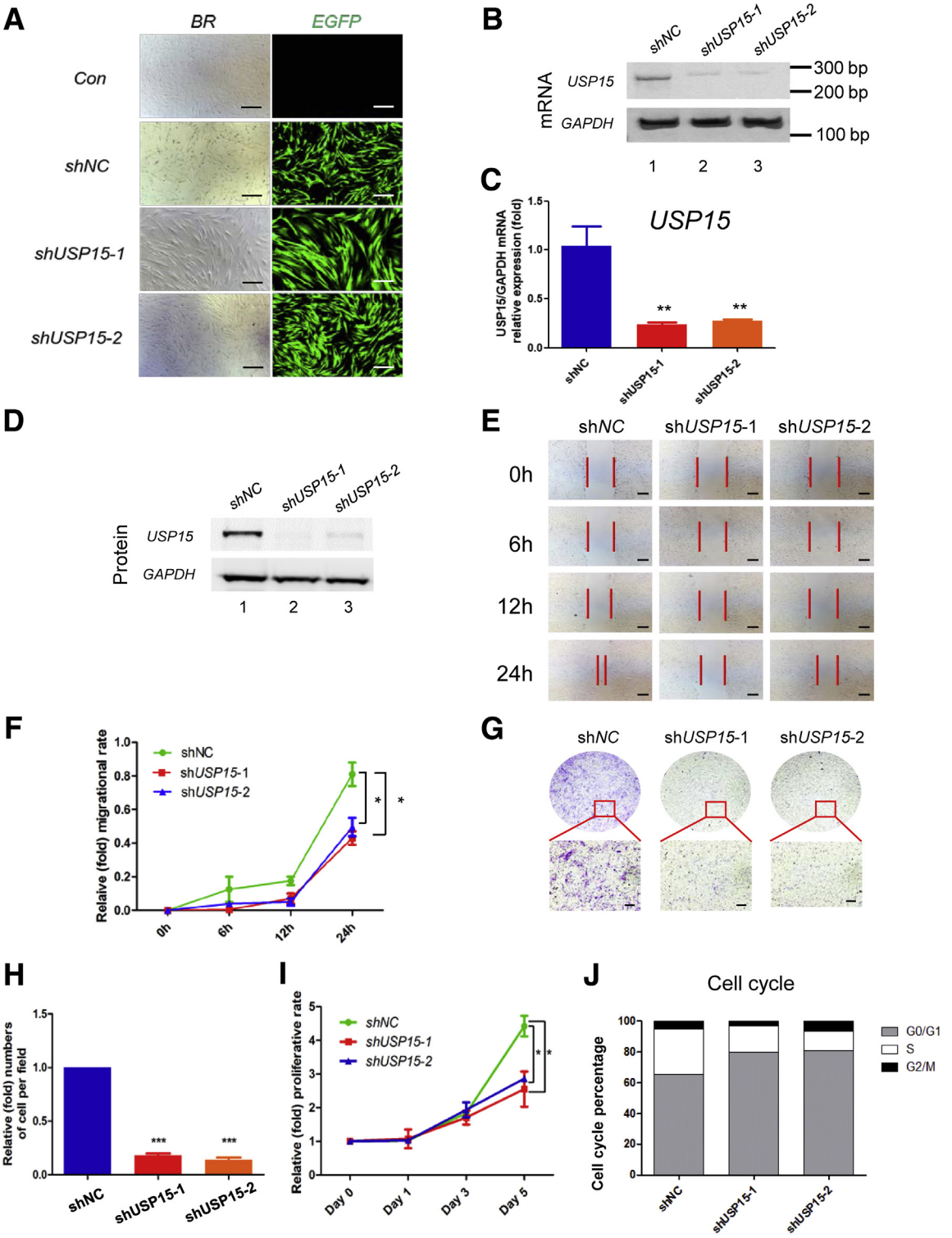

Figure 2 Knockdown of *USP15* restricts human dermal fibroblast (HDF) migration and proliferation. **A:** Validation of lentivirus transfection with enhanced green fluorescent protein (eGFP) and shUSP15-RNA into HDFs. Scramble-shRNA served as a negative control (*shNC*). **B** and **C:** Native PAGE (**B**) and quantitative real-time PCR (**C**) were performed to prove that endogenous *USP15* mRNA is silenced. **D:** Western blot analysis shows that the USP15 protein level is suppressed after transfection of shUSP15-1/2. **E:** Scratch assays show a significant inhibition of cell migration in HDFs transfected with *shUSP15-1/2* compared with that in HDFs transfected with *shNC*. Cells were imaged over 24 hours after scratching. **Red lines:** margins of cells migrated to central part. **F:** Quantification of cells that migrate to the midline of the scratch wound. **G:** Transwell assays demonstrated that *USP15* deficiency results in abrogation of cell motility. **H:** Cell numbers at three random sites on each transwell filter were counted and calculated. **I:** Cell Counting Kit-8 assays show that HDF proliferation is significantly inhibited *in vitro*. The summary data are from three independent experiments. **J:** Cell cycle arrest at the G_0/G_1 phase and a decreased proportion of cells in the S phase by flow cytometry also indicate that cell proliferation is blocked. Data are expressed as means ± SEM (**H**). $^*P < 0.05$, $^{**}P < 0.01$, and $^{***}P < 0.001$ versus *shNC*. Scale bars: 50 μm (**A** and **G**); 100 μm (**E**). BR, bright field; Con, control; GAPDH, glyceraldehyde-3-phosphate dehydrogenase.

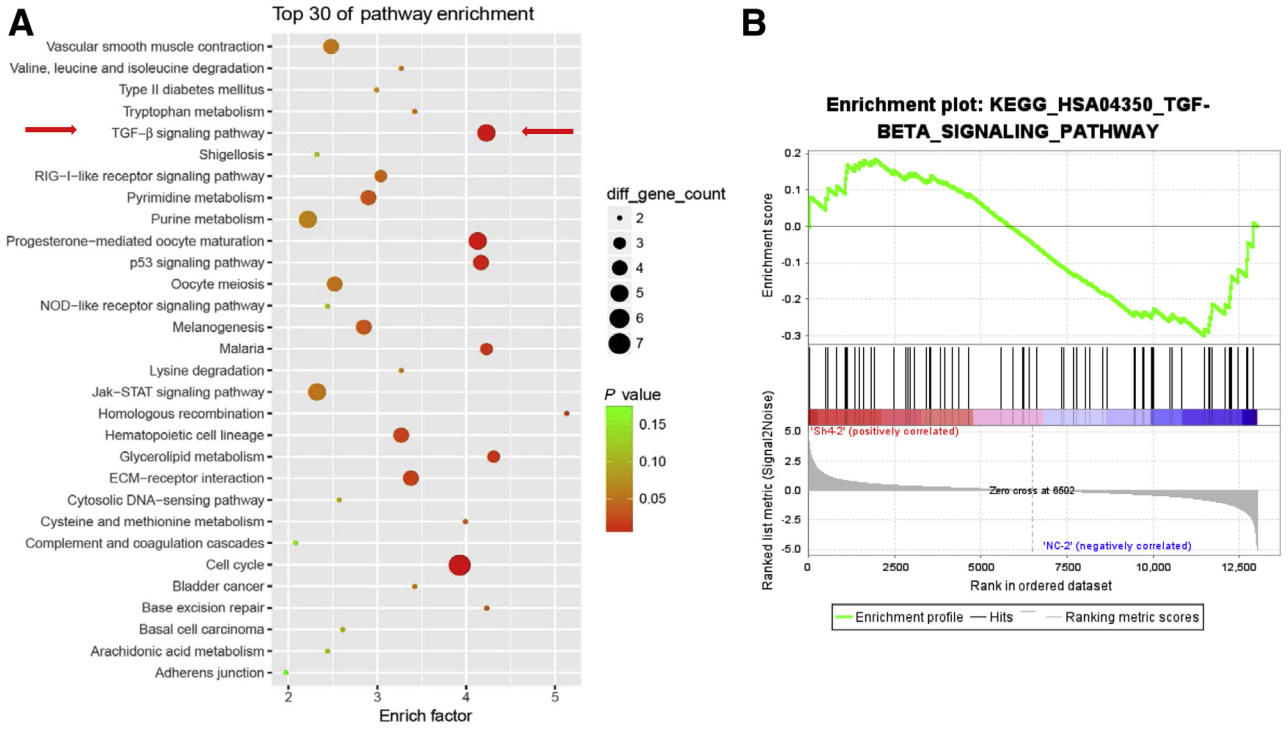

Figure 3 Transcriptional sequencing reveals that the transforming growth factor (TGF)-β signaling pathway is the major downstream pathway of USP15. **A:** RNA sequencing was performed after silencing of *USP15*. Kyoto Encyclopedia of Genes and Genomes (KEGG) pathway enrichment analysis reveals that the TGF-β pathway is significantly down-regulated. Human dermal fibroblasts transfected with scramble-shRNA served as a negative control. **B:** Gene Set Enrichment Analysis reveals a dynamic change and inhibition of TGF-β pathway intensity. $P < 0.05$. diff_gene_count, differential expressed gene number counts; ECM, extracellular matrix; Jak, Janus kinase; NOD, nucleotide binding oligomerization domain; RIG1, retinoic acid inducible gene 1.

indicated that HDF migration was reduced in the USP15 knockdown group (Figure 2, G and H). Cell Counting Kit-8 assays demonstrated that USP15 knockdown significantly inhibited cell proliferation (Figure 2I). As shown by flow cytometry, the cell cycle was arrested at the G_0/G_1 phase, with a decreased proportion of cells in the S phase, after inhibition of USP15 expression (Figure 2J), which further confirmed that the absence of USP15 blocked cell proliferation. Taken together, these results suggest that HDF cellular viability was remarkably restricted under USP15-deficient conditions. Hence, it is important to investigate how USP15 promotes wound healing.

Silencing USP15 Attenuates the TGF-β Pathway

To identify the pathways and factors downstream of USP15, RNA-sequencing analysis was performed using HDFs transfected with USP15-shRNA and scramble-shRNA. Kyoto Encyclopedia of Genes and Genomes pathway enrichment analysis showed that the TGF-β pathway was significantly down-regulated ($P < 0.05$) (Figure 3A). Furthermore, on the basis of Gene Set Enrichment Analysis, significant repression of the TGF-β signaling pathway was observed in *USP15*-suppressed HDFs (Figure 3B). Thus, in subsequent experiments, the effects of USP15 were studied on the TGF-β pathway.

USP15 Maintains TGF-β Levels Both *in Vivo* and *in Vitro*

Because USP15 could regulate TGF-β, TGF-β1 levels and the expression of other related targets were tested in *Usp15*-deficient mice and HDFs. First, reduced TGF-β1 levels, compared with those of WT mice, were observed in the peripheral blood of *Usp15*-deleted mice by enzyme-linked immunosorbent assay (Figure 4A). In addition, *Usp15*-deleted mice expressed less TGF-β1 and *TBR1* mRNA than WT mice in wounded skin (Figure 4B). In wounds from WT mice, *Tgfb1* mRNA was significantly up-regulated through day 3 and day 5, whereas in USP15 KO mice, there was no significant change in this gene during wound healing. However, compared with wounded skin from WT mice, *Usp15*-deficient skin showed a significant decrease in *Tgfb1* mRNA. The *in vivo* experiments also showed a lower *TBR1* mRNA level in wounded skin from *Usp15* KO mice than in WT skin from day 1 to day 5.

The expression of the TBR1 and the TGF-β1 target gene PAI1 was assessed in HDFs *in vitro*. As expected, SERPINE1 and TBR1 were decreased at both the mRNA (Figure 4C) and protein (Figure 4E) levels after silencing of USP15. A reduction in *TGFB1* and *SERPINE1* mRNA levels was also observed in cells transfected with shUSP15-RNAs (Figure 4D). Moreover, to evaluate the effect of USP15 on TGF-β signaling

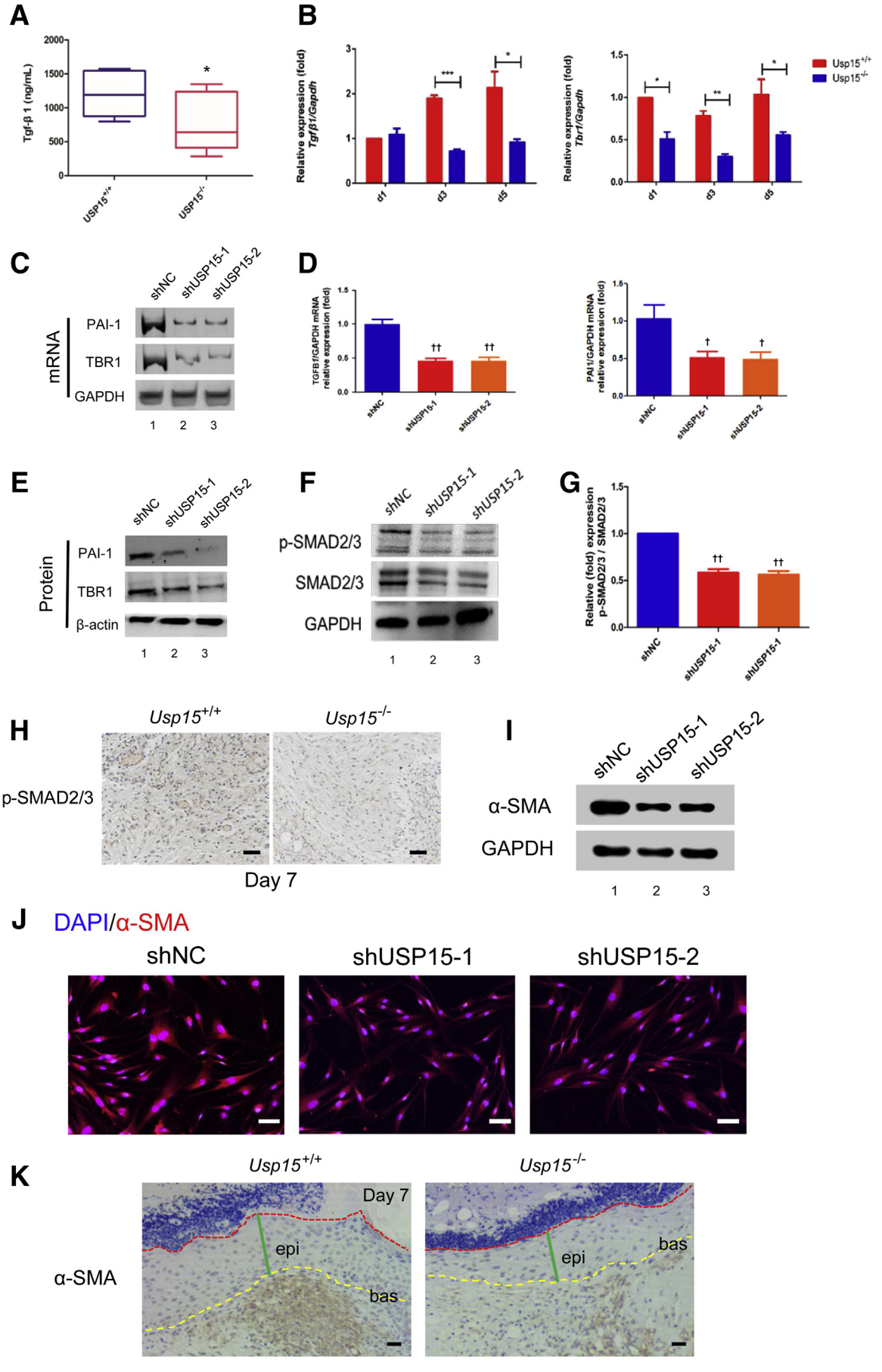
A
Tgf-β 1 (ng/mL)
2000
1500
1000
500
0
*
USP15+/+
USP15-/-
B
Relative expression (fold)
Tgfβ1/Gapdh
***
*
d1
d3
d5
Relative expression (fold)
Tbr1/Gapdh
*
**
*
Usp15+/+
Usp15-/-
C
shNC
shUSP15-1
shUSP15-2
mRNA
PAI-1
TBR1
GAPDH
1 2 3
D
TGFB1/GAPDH mRNA relative expression (fold)
††
††
shNC
shUSP15-1
shUSP15-2
PAI1/GAPDH mRNA relative expression (fold)
†
†
E
shNC
shUSP15-1
shUSP15-2
Protein
PAI-1
TBR1
β-actin
1 2 3
F
shNC
shUSP15-1
shUSP15-2
p-SMAD2/3
SMAD2/3
GAPDH
1 2 3
G
Relative (fold) expression p-SMAD2/3 / SMAD2/3
††
††
shNC
shUSP15-1
shUSP15-1
H
Usp15+/+
Usp15-/-
p-SMAD2/3
Day 7
I
shNC
shUSP15-1
shUSP15-2
α-SMA
GAPDH
1 2 3
J
DAPI/α-SMA
shNC
shUSP15-1
shUSP15-2
K
Usp15+/+
Usp15-/-
α-SMA
Day 7
epi
bas
epi
bas

pathway activity, the level of phosphorylated SMAD2/3, which acts as the main mediator of TGF-β signaling, was examined in both negative control and shUSP15-transfected cells. Decreased levels of phosphorylated SMAD2/3 in USP15 knockdown HDFs resulted in a weakened signaling intensity of the TGF-β pathway (Figure 4, F and G). Immunohistochemical staining of phosphorylated Smad2/3 was further confirmed in *USP15* WT/KO mice (Figure 4H). This result was consistent with the *in vitro* finding that SMAD2/3 phosphorylation was reduced in $Usp15^{-/-}$ mice.

Moreover, α-smooth muscle actin (α-SMA) was tested in both USP15-silenced and control HDFs by Western blot analysis (Figure 4I) and immunofluorescence (Figure 4J). The results showed that α-SMA significantly decreased after knocking down USP15 *in vitro*. Similarly, immunohistochemical staining of α-SMA also revealed reduced expression of α-SMA in the skin of $Usp15^{-/-}$ mice compared with that in wild-type mice (Figure 4K). Thus, myofibroblast induction was impaired after silencing of USP15 both *in vitro* and *in vivo*.

USP15 Binds to the SMAD Protein Family

After exploring the biological function of USP15 in HDFs, it was subsequently assessed in detail how USP15 regulates TGF-β signaling. Given that USP15 is a DUB for receptor-activated SMADs, it was tested whether the SMAD protein family, including SMAD1/5, SMAD2/3, SMAD4, and SMAD7, could form a complex with USP15 under conditions with or without exogenous recombinant human TGF-β1.

The Co-IP assays showed that USP15 could coimmunoprecipitate with SMAD2/3, SMAD4, and SMAD7 but not SMAD1/5 in HDFs (Figure 5A). However, endogenous *USP15* had a higher affinity for endogenous SMAD7 than other SMAD proteins under physiological conditions (Figure 5A). Moreover, only SMAD7 dissociated from USP15 after treatment with a high concentration of exogenous recombinant human TGF-β1 (100 ng/mL). Thus, the intensity of TGF-β could directly influence the formation of the USP15-SMAD7 complex.

The USP15/SMAD7 Complex Binds to TBR1 and Inhibits Its Ubiquitination

According to the results above, the conclusions were verified by immunofluorescence, and the results were in accordance with those obtained in the coimmunoprecipitation assay. USP15 and SMAD7 were colocalized under TGF-β1−deprived conditions (Figure 5B). Nevertheless, when stimulated with 100 ng/mL exogenous recombination TGF-β1, USP15 dissociated from SMAD7, generating two isolated peaks for the red and green signals (Figure 5B).

Because SMAD7 binds to TBR1, it was next explored whether SMAD7 could also bind to TBR1 in HDFs. As expected, TBR1 strongly interacted with SMAD7 (Figure 5C). Combined with the above results showing that USP15 forms a complex with SMAD7, we hypothesized that USP15 could be recruited to TBR1 by SMAD7. A Co-IP assay demonstrated that USP15 interacted with TBR1 and that endogenous USP15 coimmunoprecipitated with endogenous TBR1 under physiological conditions. In the presence of a high concentration of TGF-β1, USP15 dissociated from SMAD7 and TBR1, whereas SMAD7 still bound to TBR1 (Figure 5, C and D). In addition, knockdown of USP15 resulted in diminished ubiquitin coimmunoprecipitation with TBR1, which indicates increased TBR1 ubiquitination (Figure 5E). Conclusively, our results illustrate that USP15 binds to SMAD7 and deubiquitinates TBR1, stabilizing the TBR1 structure. This change results in maintenance of TGF-β signaling pathway activity, leading to an acceleration of wound repair (Figure 5F).

Discussion

Wound healing is a process of cutaneous barrier reconstruction in which the skin and the connective tissues remodel themselves after injury. Typically, the process is divided into predictable phases: blood clotting (hemostasis), inflammation, tissue growth (proliferation), and tissue remodeling (maturation). In the last two phases, activated dermal fibroblasts rebuild the tissue scaffold for cutaneous regeneration.[19] A previous study showed that bone morphogenetic protein 2 (*BMP2*) can directly promote HDF

Figure 4 USP15 regulates the transforming growth factor (TGF)-β pathway both *in vivo* and *in vitro*. **A:** An enzyme-linked immunosorbent assay shows that the endogenous TGF-β1 level in the peripheral blood of $USP15^{-/-}$ mice is lower than that in wild-type mice. **B:** TGF-β1 mRNA levels in wounded skin are decreased at day 3 and day 5 compared with those of the wild type. TGF-β receptor I (TBR1) mRNA expression was also diminished compared with that of the wild type. **C:** Native PAGE shows decreased *TBR1* and serpin family E member 1 (*SERPINE1*) mRNA levels in USP15 knockdown human dermal fibroblasts (HDFs). **D:** Quantitative real-time PCR results show that the mRNA levels of TGF-β1 and its target gene *SERPINE1* are both significantly decreased when USP15 is silenced. **E:** Western blot analysis of HDFs shows that TBR1 and *SERPINE1* protein expression is down-regulated in cells transfected with shUSP15. **F** and **G:** SMAD2/3 phosphorylation (p-SMAD2/3) is significantly inhibited in USP15-deficient HDFs, whereas total SMAD2/3 is not significantly changed, as shown by Western blot analysis. Total SMAD2/3 was used as the internal control. **H:** Immunohistochemical (IHC) staining of p-SMAD2/3 in *Usp15* wild-type/knockout (WT/KO) mice. SMAD2/3 phosphorylation is depressed in $Usp15^{-/-}$ mice. **I:** Western blot analysis shows decreased α-smooth muscle actin (α-SMA) expression in HDFs after knockdown of USP15. **J:** Immunofluorescence reveals a weaker α-SMA signal in USP15-silenced HDFs. **K:** IHC staining of α-SMA in *Usp15* WT/KO mice. **Yellow dashed lines** indicate basal layer (bas); **red dashed lines**, epidermis; **green lines**, thickness of the epidermis (epi). $^{*}P < 0.05$, $^{**}P < 0.01$, and $^{***}P < 0.001$ versus $USP15^{+/+}$ (unpaired *t*-test); $^{\dagger}P < 0.05$, $^{\dagger\dagger}P < 0.01$ versus shNC. Scale bar = 50 μm (**J** and **K**). GAPDH, glyceraldehyde-3-phosphate dehydrogenase; shNC, scramble-shRNA served as a negative control.

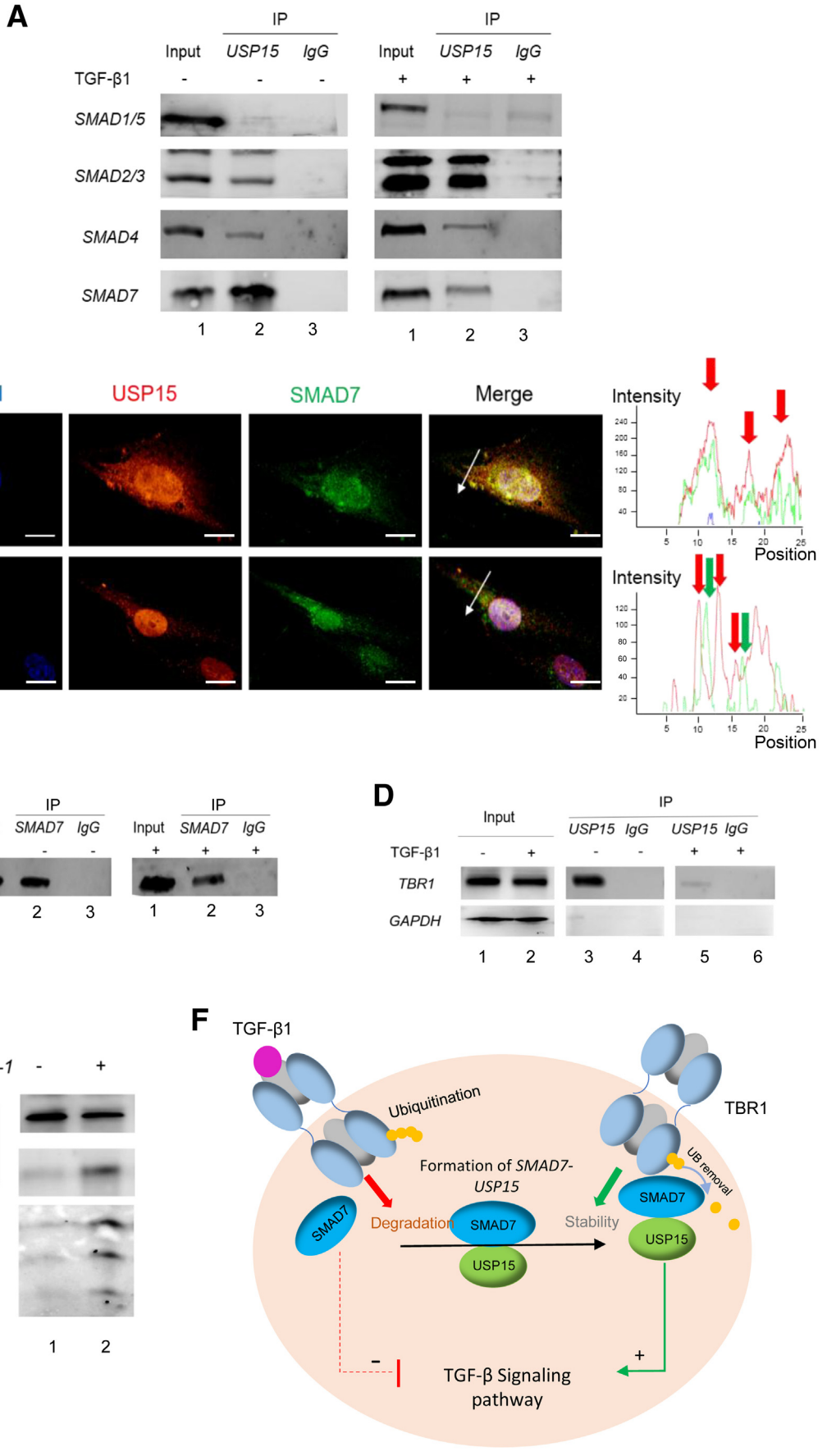
A
IP
Input
USP15
IgG
TGF-β1
SMAD1/5
SMAD2/3
SMAD4
SMAD7
1 2 3
B
DAPI
USP15
SMAD7
Merge
TGF-β
Intensity
Position
C
TBR1
D
TBR1
GAPDH
1 2 3 4 5 6
E
shUSP15-1
Input
IP:UB
IP:TBR1
UB
F
TGF-β1
Ubiquitination
TBR1
Formation of SMAD7-USP15
UB removal
Degradation
Stability
TGF-β Signaling pathway

proliferation and migration with activated ECM reconstruction, thereby accelerating wound healing.[20] However, whether USP15 plays a key role in the activation of HDFs during wound healing remains largely unknown. Herein, we first revealed that USP15 could promote wound healing by enhancing the proliferation and migration of HDFs and activating the TGF-β signaling pathway, thereby providing a novel therapeutic target for the treatment of refractory wounds.

USP15, a DUB that removes conjugated ubiquitin from target proteins, plays a leading role in ubiquitin-dependent processes through polyubiquitin chain disassembly and hydrolysis of ubiquitin-substrate bonds. To date, this enzyme has been reported to be involved with transcriptional regulation, DNA repair, and mitophagy.[21] For example, USP15 can regulate gene expression and/or DNA repair through the deubiquitination of histone H2B.[22] Recently, USP15 was also shown to affect TGF-β signaling through the deubiquitination of receptor-activated SMAD transcription factors.[14] We demonstrate herein, for the first time, that USP15 can directly modulate wound healing by stabilizing TBR1 and maintaining the TGF-β signaling pathway, which represents a novel regulatory mechanism of USP15.

TGF-β is one of the most extensively studied signaling molecules, and the role of TGF-β1 as a proponent of wound healing is well characterized.[23,24] To date, numerous factors have been revealed to regulate TGF-β1 RNA and protein expression, such as thrombospondin-1, BMPs, and SMADs.[25,26] TGF-β receptors have also been reported to be involved in various post-translational modifications, such as phosphorylation and ubiquitination.[27] Previous studies have confirmed that USP15 can also deubiquitinate and stabilize TBR1 in an SMAD7-dependent manner.[28] Herein, we confirmed that this theory could be applied to wound healing, which provides an alternative explanation for post-translational modifications of the TGF-β receptor during cutaneous wound repair.

Myofibroblast induction is mainly characterized by up-regulated expression of α-SMA and enhanced ECM synthesis compared with typical fibroblasts.[29] During wound healing, myofibroblast induction is activated by the TGF-β signaling pathway, causing increased motility of fibroblast cells and accelerated fibrosis.[30] Herein, for the first time, we reported that USP15 promoted the differentiation of fibroblasts into myofibroblasts, which reconstructed the ECM in the wound area and activated cell motility, causing accelerated cutaneous wound repair.

Skin wound healing requires diverse cell types, such as macrophages, activated T/B lymphocytes, and keratinocytes.[31,32] Further investigations could explore the regulatory roles of USP15 in these cells during skin wound repair. Only one HDF cell strain was assessed in this study, which might not provide representative evidence. We will examine whether USP15 can regulate TGF-β signaling in primary fibroblasts with diverse origins in a subsequent study.

Rodent skin does not heal by epidermal migration alone. Wound healing is simultaneously regulated by epidermal migration and contraction. In our study, the measured wound area could be influenced by both migration and contraction. Further studies should explore the role of USP15 in epidermal migration and contraction. In addition, there is a fundamental difference in wound healing between mice and humans, as contraction is the primary mechanism for murine skin repair,[33] and further studies could explore the clinical applications of treating refractory wounds via supplementation with the recombinant *USP15* protein.

Thus, it was concluded that silencing *USP15* attenuates TGF-β/Smad signaling intensity and subsequently results in dysfunctional wound healing. More specifically, our research proves that USP15 directly deubiquitinates TGF-β receptor I to promote wound healing. Because of the druggable enzymatic activity of DUBs, USP15 is considered a potential therapeutic target with important clinical applications.[34] Recombinant DUBs can be applied to accelerate wound repair, whereas small molecules targeting DUBs may become a new intervention for cutaneous overhealing outcomes, such as keloids and hypertrophic scars.[35,36] Further studies on the effects of *USP15* overexpression will be performed in the future to assess the full functions of USP15 in wound healing.

Acknowledgment

We thank Dr. Peiwei Chai for his support.

Figure 5 USP15 deubiquitinates transforming growth factor (TGF)-β receptor I (TBR1) by forming a complex with SMAD7 and TBR1. **A:** Immunoprecipitation (IP) of USP15 in human dermal fibroblasts (HDFs) treated with or without 100 ng/mL recombinant human TGF-β1 for 24 hours and immunoblot assays of SMAD1/5, SMAD2/3, SMAD4, and SMAD7. USP15 binds to SMAD2/3, SMAD4, and SMAD7 under physiological conditions, but only SMAD7 dissociates from USP15 in the presence of high concentrations of TGF-β1. **B: Left panels:** Immunofluorescence assays of USP15 (red) and SMAD7 (green) in HDFs treated with TGF-β1. **Right panel:** The red and green signals are overlapping in the normal culture environment, whereas they are separated from each other in the high TGF-β1 environment. Fluorescence intensity was quantified according to the **white arrows**. **Green arrows** indicate SMAD7 immunofluorescence intensity; **red arrows**, USP15 immunofluorescence intensity. **C:** Coimmunoprecipitation assays confirm that SMAD7 and TBR1 bind to each other in the presence or absence of exogenous TGF-β1. **D:** Immunoprecipitation of USP15 and immunoblotting of TBR1 show that USP15 can form a complex with TBR1 and dissociate from TBR1 after treatment with exogenous TGF-β1. **E:** Coimmunoprecipitation assays of ubiquitin (UB) and TBR1 in HDFs transfected with shUSP15 and scramble-shRNA that served as a negative control negative control. Silencing USP15 promotes TBR1 ubiquitination. **F:** Schematic of USP15-mediated regulation of the TGF-β pathway. SMAD7 recruits USP15, and the USP15-SMAD7 complex stabilizes the structure of TBR1 by decreasing TBR1 ubiquitination. TBR1 stabilization is enhanced and, thus, strengthens the TGF-β signaling pathway. Scale bars = 10 μm (**B**).

References

1. Gurtner GC, Werner S, Barrandon Y, Longaker MT: Wound repair and regeneration. Nature 2008, 453:314–321
2. Pikula M, Langa P, Kosikowska P, Trzonkowski P: [Stem cells and growth factors in wound healing] Polish. Postepy Hig Med Dosw 2015, 69:874–885
3. Driskell RR, Watt FM: Understanding fibroblast heterogeneity in the skin. Trends Cell Biol 2015, 25:92–99
4. Stunova A, Vistejnova L: Dermal fibroblasts: a heterogeneous population with regulatory function in wound healing. Cytokine Growth Factor Rev 2018, 39:137–150
5. Finnson KW, McLean S, Di Guglielmo GM, Philip A: Dynamics of transforming growth factor beta signaling in wound healing and scarring. Adv Wound Care (New Rochelle) 2013, 2:195–214
6. Penn JW, Grobbelaar AO, Rolfe KJ: The role of the TGF-beta family in wound healing, burns and scarring: a review. Int J Burns Trauma 2012, 2:18–28
7. Pakyari M, Farrokhi A, Maharlooei MK, Ghahary A: Critical role of transforming growth factor beta in different phases of wound healing. Adv Wound Care (New Rochelle) 2013, 2:215–224
8. Sorokin AV, Kim ER, Ovchinnikov LP: Proteasome system of protein degradation and processing. Biochemistry (Mosc) 2009, 74: 1411–1442
9. Aggarwal K, Massague J: Ubiquitin removal in the TGF-beta pathway. Nat Cell Biol 2012, 14:656–657
10. Qiu GZ, Sun W, Jin MZ, Lin J, Lu PG, Jin WL: The bad seed gardener: deubiquitinases in the cancer stem-cell signaling network and therapeutic resistance. Pharmacol Ther 2017, 172:127–138
11. Rape M: Ubiquitylation at the crossroads of development and disease. Nat Rev Mol Cell Biol 2018, 19:59–70
12. Mevissen TET, Komander D: Mechanisms of deubiquitinase specificity and regulation. Annu Rev Biochem 2017, 86:159–192
13. Baker RT, Wang XW, Woollatt E, White JA, Sutherland GR: Identification, functional characterization, and chromosomal localization of USP15, a novel human ubiquitin-specific protease related to the UNP oncoprotein, and a systematic nomenclature for human ubiquitin-specific proteases. Genomics 1999, 59:264–274
14. Inui M, Manfrin A, Mamidi A, Martello G, Morsut L, Soligo S, Enzo E, Moro S, Polo S, Dupont S, Cordenonsi M, Piccolo S: USP15 is a deubiquitylating enzyme for receptor-activated SMADs. Nat Cell Biol 2011, 13:1368–1375
15. Villeneuve NF, Tian W, Wu T, Sun Z, Lau A, Chapman E, Fang D, Zhang DD: USP15 negatively regulates Nrf2 through deubiquitination of Keap1. Mol Cell 2013, 51:68–79
16. Zou Q, Jin J, Hu H, Li HS, Romano S, Xiao Y, Nakaya M, Zhou X, Cheng X, Yang P, Lozano G, Zhu C, Watowich SS, Ullrich SE, Sun SC: USP15 stabilizes MDM2 to mediate cancer-cell survival and inhibit antitumor T cell responses. Nat Immunol 2014, 15:562–570
17. Torre S, Polyak MJ, Langlais D, Fodil N, Kennedy JM, Radovanovic I, Berghout J, Leiva-Torres GA, Krawczyk CM, Ilangumaran S, Mossman K, Liang C, Knobeloch KP, Healy LM, Antel J, Arbour N, Prat A, Majewski J, Lathrop M, Vidal SM, Gros P: USP15 regulates type I interferon response and is required for pathogenesis of neuroinflammation. Nat Immunol 2017, 18:54–63
18. Liang X, Chai B, Duan R, Zhou Y, Huang X, Li Q: Inhibition of FKBP10 attenuates hypertrophic scarring through suppressing fibroblast activity and extracellular matrix deposition. J Invest Dermatol 2017, 137:2326–2335
19. Driskell RR, Lichtenberger BM, Hoste E, Kretzschmar K, Simons BD, Charalambous M, Ferron SR, Herault Y, Pavlovic G, Ferguson-Smith AC, Watt FM: Distinct fibroblast lineages determine dermal architecture in skin development and repair. Nature 2013, 504: 277–281
20. Ishihara A, Zekas LJ, Litsky AS, Weisbrode SE, Bertone AL: Dermal fibroblast-mediated BMP2 therapy to accelerate bone healing in an equine osteotomy model. J Orthop Res 2010, 28:403–411
21. Cornelissen T, Haddad D, Wauters F, Van Humbeeck C, Mandemakers W, Koentjoro B, Sue C, Gevaert K, De Strooper B, Verstreken P, Vandenberghe W: The deubiquitinase USP15 antagonizes Parkin-mediated mitochondrial ubiquitination and mitophagy. Hum Mol Genet 2014, 23:5227–5242
22. Long L, Thelen JP, Furgason M, Haj-Yahya M, Brik A, Cheng D, Peng J, Yao T: The U4/U6 recycling factor SART3 has histone chaperone activity and associates with USP15 to regulate H2B deubiquitination. J Biol Chem 2014, 289:8916–8930
23. Sefat F, Denyer MC, Youseffi M: Effects of different transforming growth factor beta (TGF-beta) isomers on wound closure of bone cell monolayers. Cytokine 2014, 69:75–86
24. Mandapalli PK, Labala S, Jose A, Bhatnagar S, Janupally R, Sriram D, Venuganti VV: Layer-by-layer thin films for co-delivery of TGF-beta siRNA and epidermal growth factor to improve excisional wound healing. AAPS PharmSciTech 2017, 18:809–820
25. Qin H, Qu C, Yamaza T, Yang R, Lin X, Duan XY, Akiyama K, Liu Y, Zhang Q, Chen C, Chen Y, Qi HH, Feng XH, Le AD, Shi S: Ossifying fibroma tumor stem cells are maintained by epigenetic regulation of a TSP1/TGF-beta/SMAD3 autocrine loop. Cell Stem Cell 2013, 13:577–589
26. Cunha SI, Magnusson PU, Dejana E, Lampugnani MG: Deregulated TGF-beta/BMP signaling in vascular malformations. Circ Res 2017, 121:981–999
27. Foot N, Henshall T, Kumar S: Ubiquitination and the regulation of membrane proteins. Physiol Rev 2017, 97:253–281
28. Eichhorn PJ, Rodon L, Gonzalez-Junca A, Dirac A, Gili M, Martinez-Saez E, Aura C, Barba I, Peg V, Prat A, Cuartas I, Jimenez J, Garcia-Dorado D, Sahuquillo J, Bernards R, Baselga J, Seoane J: USP15 stabilizes TGF-beta receptor I and promotes oncogenesis through the activation of TGF-beta signaling in glioblastoma. Nat Med 2012, 18: 429–435
29. Hrycaj SM, Marty-Santos L, Cebrian C, Rasky AJ, Ptaschinski C, Lukacs NW, Wellik DM: Hox5 genes direct elastin network formation during alveologenesis by regulating myofibroblast adhesion. Proc Natl Acad Sci U S A 2018, 115:E10605–E10614
30. Shook BA, Wasko RR, Rivera-Gonzalez GC, Salazar-Gatzimas E, Lopez-Giraldez F, Dash BC, Munoz-Rojas AR, Aultman KD, Zwick RK, Lei V, Arbiser JL, Miller-Jensen K, Clark DA, Hsia HC, Horsley V: Myofibroblast proliferation and heterogeneity are supported by macrophages during skin repair. Science 2018, 362. eaar2971
31. Rognoni E, Watt FM: Skin cell heterogeneity in development, wound healing, and cancer. Trends Cell Biol 2018, 28:709–722
32. Schmidt BA, Horsley V: Intradermal adipocytes mediate fibroblast recruitment during skin wound healing. Development 2013, 140: 1517–1527
33. Dunn L, Prosser HC, Tan JT, Vanags LZ, Ng MK, Bursill CA: Murine model of wound healing. J Vis Exp 2013, 75:e50265
34. He M, Zhou Z, Wu G, Chen Q, Wan Y: Emerging role of DUBs in tumor metastasis and apoptosis: therapeutic implication. Pharmacol Ther 2017, 177:96–107
35. Piao J, Tashiro A, Nishikawa M, Aoki Y, Moriyoshi E, Hattori A, Kakeya H: Expression, purification and enzymatic characterization of a recombinant human ubiquitin-specific protease 47. J Biochem 2015, 158:477–484
36. Lee BH, Lee MJ, Park S, Oh DC, Elsasser S, Chen PC, Gartner C, Dimova N, Hanna J, Gygi SP, Wilson SM, King RW, Finley D: Enhancement of proteasome activity by a small-molecule inhibitor of USP14. Nature 2010, 467:179–184